Global Earthing System: Can Buried Metallic Structures Significantly Modify the Ground Potential Profile?

Global Earthing System: Can Buried Metallic Structures Significantly Modify the Ground Potential Profile?

E. Pons, P. Colella, R. Tommasini, R. Napoli
Members, IEEE
Politecnico di Torino Dipartimento Energia
C.so Duca degli Abruzzi, 24, 10129 Torino, ITALY
enrico.pons@polito.it
pietro.colella@polito.it
riccardo.tommasini@polito.it
roberto.napoli@polito.it

P. Montegiglio, G. Cafaro, F. Torelli
Politecnico di Bari
Dipartimento di Ingegneria Elettrica e dell'Informazione
Via Orabona, 4, 70125 Bari, ITALY
pasqualemontegiglio@gmail.com
giuseppe.cafaro@poliba.it
francesco.torelli@poliba.it

Abstract **-- Global Earthing Systems (GESs), created by the interconnection of local Earthing Systems (ESs), should guarantee the absence of dangerous touch voltages. According to international Standards, one of the reasons for this safety characteristic of GESs is that MV and LV grounding systems form a quasi-equipotential area. Typical examples of GESs are in city centers, thanks to the high number of interconnected grounding systems in the area. For this reason, in addition to ground-grids, also other metallic parts with different primary functions shall be considered: for example, water and gas pipes, tramway tracks and building foundations can modify the electric potential distribution in the area.**

In this paper, a model based on the Maxwell's sub-areas method (MaSM) is used to evaluate how buried metallic parts, not intentionally connected to ground-grids, modify the electric potential on the soil surface.

Firstly, the MaSM model is validated with experimental measurements on a simple electrodes configuration. The measured voltages are compared with the MaSM results and with the results obtained with a FEM model simulated with COMSOL Multiphysics.

Then the simulations are carried out on a realistic urban test case.

Index Terms**-- Electrical safety, GES, Global Earthing System, grounding, ground potential, ground rod, interference, Maxwell's sub-areas method, MV fault, transferred potentials.**

I. NOMENCLATURE

DSO = Distribution System Operator
ES = Earthing System;
GES = Global Earthing System;
EPR = Earth Potential Rise;
PEP = Passive Electrode Potential
FEM = Finite Element Method
MaSM = Maxwell's Sub-Areas Method
MV = Medium Voltage
LV = Low Voltage
TP = Transferred Potential
U_{vT} = Prospective Touch Voltage

This work was supported in part by the Italian CCSE (Cassa Conguaglio per il Settore Elettrico), in the framework of the Meterglob project.

II. INTRODUCTION

The international and European standards IEC EN 61936-1 [1] and EN 50522 [2] define a Global Earthing System (GES) as an "equivalent earthing system created by the interconnection of local Earthing Systems (ESs) that ensures, by the proximity of the earthing systems, that there are no dangerous touch voltages". The same standards explain in the notes that "Such systems permit the division of the earth fault current in a way that results in a reduction of the earth potential rise (EPR) at the local earthing system. Such a system could be said to form a quasi-equipotential surface" and that "the existence of a global earthing system may be determined by sample measurements or calculation for typical systems. Typical examples of global earthing systems are in city center; urban or industrial areas with distributed low- and high-voltage earthing".

If an ES is part of a GES, there are some technical and economic advantages for MV users and Distribution System Operators (DSOs). In fact Standard EN 50522 [2] considers that if the relevant installation becomes a part of a global earthing system, the permissible touch voltage values, that normally need to be verified [3], are automatically respected. As far as concerns testing activities, it further states that: "Proof of touch voltage, if necessary, is to be made by measurement or calculation. Inside the global earthing system areas there is no need to verify the resistance to earth or the earth potential rise because a basic design of earthing system is sufficient".

Nevertheless, Standards do not provide a pre-defined practical procedure to certify the presence of a GES.

From the GES definition, two phenomena emerge: the first is the distribution of the earth fault current among the interconnected ES [4], [5] and the second is the creation of a quasi-equipotential surface [6], [7]. Until today, neither of them is supported by scientific evidences. In this paper, we focus on the second aspect.

Standards IEC EN 61936-1 [1] and EN 50522 [2] consider MV and LV grounding systems as buried metallic parts that

actively contribute to the achievement of a quasi-equipotential area. In urban areas however also other metallic parts, with different primary functions, shall be contemplated. For example, water and gas pipes, tramway tracks and building foundations can significantly modify the electric potential distribution in an area. If they are joined to the main grounding terminal of the buildings that they supply, as recommended by IEC 60364-4 [8], they can function as a connection between ESs. If they are not joined to ESs but only buried in their area of influence and directly in contact with the ground, they can however contribute to modify the ground surface potential profile.

Several papers have investigated the risk of electric shock due to the coupling of an ES with metallic parts which can transfer dangerous potentials from the leaking (or "active") grid, to "passive" grids in other areas [9]–[12].

For the cases that they analyze, they correctly consider the potential transfer as a source of risk. In the particular context evaluated in this paper (urban area with a possible GES), where the buried metallic parts are several and close to one another, the transferred potential can be a positive phenomenon, as it can contribute to achieve the quasi-equipotential area cited by the standards [1], [2], thus decreasing the touch voltages.

The objective of this paper is to evaluate how buried metallic parts, which interfere with a grounding system injecting a fault current into the ground, modify the ground electric potential profile, with the purpose of assessing if the equipotentialization effect in a GES cited by standards [1], [2] is considerable or negligible.

A model based on the Maxwell's sub-areas method was implemented. A short description of the model is given in paragraph III, pointing out strengths and weaknesses. In order to validate the model, experimental measurements were carried out on a simple configuration. The measured values are compared with the Maxwell's sub-areas model results and with the results obtained through a FEM model simulated with COMSOL Multiphysics (paragraph IV).

The MaSM model is then used for the simulation of the injection into the ground of a fault current in an urban context, potentially candidate to be defined GES (paragraph V). Several scenarios are simulated, characterized by the presence of different buried metallic structures.

The ground surface potential distributions obtained in the different scenarios are compared with that of a base case in which only the ES of the faulted MV/LV substation is present.

III. THE MODELS: MASM & FEM

The study of a grounding system leaking a known, quasi-static, fault current I_F can be performed applying the Maxwell's subareas method [13]–[18].

According to the MaSM, a complex grounding electrode can be generally subdivided into a suitable number n of cylindrical segments, which must have a length adequately greater than their diameter and be at the same potential under fault conditions. The occurrence of the first condition allows to assume the current field generated by each segment the same as that produced by a uniform linear current source laying on its longitudinal axis. The second condition states that the voltage drop across the metallic parts of a ground electrode is negligible.

Fig. 1 shows an example of discretization of a simple cylindrical electrode embedded in a conductive homogeneous medium in n segments.

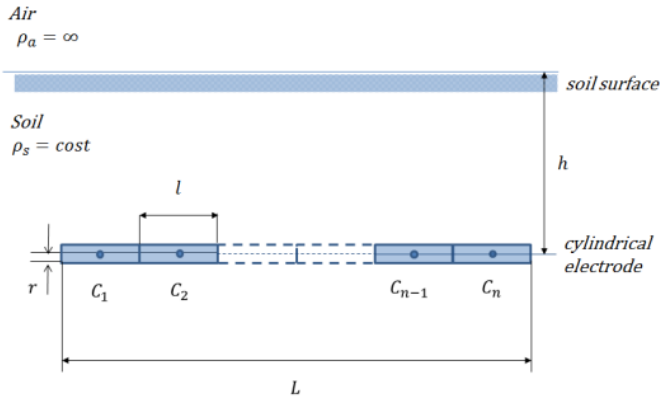

Fig. 1. Example of discretization of a simple cylindrical electrode

Every single segment interferes with the others: in a homogeneous medium of resistivity ρ, the potential of a generic segment j caused by the current I_i dispersed by the segment i of length l, is defined as:

$$V_{i,j} = \frac{\rho I_i}{4\pi l} ln \left[\frac{x + \frac{l}{2} + \sqrt{\left(x + \frac{l}{2}\right)^2 + y^2 + z^2}}{x - \frac{l}{2} + \sqrt{\left(x - \frac{l}{2}\right)^2 + y^2 + z^2}} \right] \quad (1)$$

where (x,y,z) are the coordinates of the centroid of the segment j on a local coordinate system centered on the current leaking electrode [10], [18].

By dividing (1) by the current I_i, the coefficient of proportionality $R_{i,j}$ between the potential $V_{i,j}$ and the current I_i can be calculated (2):

$$R_{i,j} = \frac{\rho}{4\pi l} ln \left[\frac{x + \frac{l}{2} + \sqrt{\left(x + \frac{l}{2}\right)^2 + y^2 + z^2}}{x - \frac{l}{2} + \sqrt{\left(x - \frac{l}{2}\right)^2 + y^2 + z^2}} \right] \quad (2)$$

Hence, considering a generic grid made of n segments, the application of the MaSM leads to the formulation of the following set of linear equations:

$$\begin{bmatrix} V_A \\ \vdots \\ V_A \\ I_F \end{bmatrix} = \begin{bmatrix} R_{1,1} & \cdots & R_{1,N} & 0 \\ \vdots & \ddots & \vdots & \vdots \\ R_{N,1} & \cdots & R_{N,N} & 0 \\ 1 & \cdots & 1 & 0 \end{bmatrix} \begin{bmatrix} I_1 \\ \vdots \\ I_N \\ 0 \end{bmatrix} \quad (3)$$

where V_A is the Earth Potential Rise (EPR) of the electrode and I_F is the leaked fault current. The n subcurrents I_j leaked by

each subarea and the EPR of the grid are the unknowns of the problem.

Knowing the subcurrents I_j allows the subsequent computation of the electric potential at any point of the soil surface.

In order to study the mutual interferences, due to proximity effects, between leaking systems and passive conductive elements (not energized independent ground-grids or extraneous conductive parts), system (3) can be easily extended [19]. The procedure consists in subdividing also the passive metallic elements, as well as the leaking systems, into subareas, and in considering each leaking system and each metallic element as a separate grounding electrode, active or passive, according to whether it leaks current or not.

Therefore, considering a generic scenario in which an active and a passive electrodes are present, respectively subdivided in N and M segments, the system of equations (4) can be written.

The presence of air in half of the space domain, as well as the presence in the medium of layers with different resistivity (multi-layer soil model), is taken into account by means of the electrical images principle [20].

The MaSM operates under the assumption of equipotentiality for grounding electrodes in steady state fault conditions. As a consequence, the use of this method leads to results whose accuracy degree decreases with increasing electrodes dimensions (long buried metal pipes, railway tracks, etc.), being the voltage drop along them no longer negligible [21].

It is possible to extend the applicability of the MaSM to the case of long buried conductors [19], [21]. The insight is to consider each of the conductors subdivisions (sub-areas or trunks) as separate grounding electrodes, connected to the trunks immediately before and after by means of an admittance.

At industrial frequency, the interference phenomenon between bare conductors in contact with the soil can be described with sufficient accuracy through purely resistive parameters [21]; so, for the above-mentioned extension, the admittance that connects the consecutive trunks can be substituted by a conductance, whose value is given by the material and section of the conductor itself, Fig. 2.

In this way, the currents flowing from a trunk to the neighboring ones became new variables and can be determined together with the leakage current distribution along conductors [19].

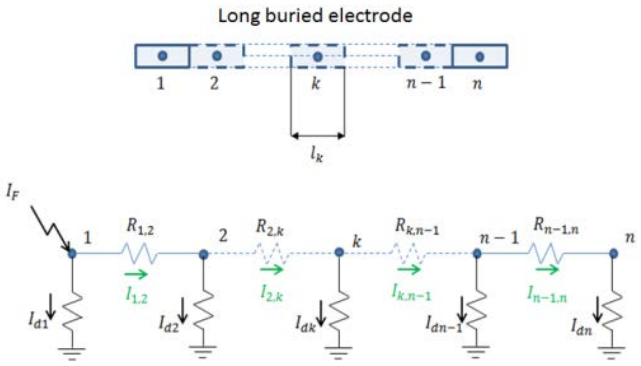

Fig. 2. Model of long electrodes

Another method to investigate the behavior of ESs is the FEM [22]. The FEM on one hand allows to overcome the simplifying hypotheses imposed by the MaSM, such as considering the soil as an infinite, flat, isotropic medium. On the other hand, modeling with FEM a vast domain in which objects with negligible width and depth are buried, such as earth conductors, become quite arduous.

In this paper, a FEM model and the experimental measurements are used to validate the MaSM model on a simple system of buried electrodes. The MaSM model, that allows the simulation of bigger systems of electrodes, is then applied to test cases that are more complicated.

IV. Model Validation

The experimental measurements for model validation were realized in a rural area called Sessant (Asti, Piemonte, Italy), where electromagnetic noises can be considered negligible and metallic buried parts are absent.

Firstly a soil characterization was done through the Wenner method.

Two electrodes were then buried, close to one another: the first one injected a current of 1 A into the soil (active electrode) while the second was kept floating (passive electrode). We measured the electric potential on both of them, and on several points on the ground surface.

More details are reported in the following paragraphs.

$$\begin{bmatrix} V_A \\ \vdots \\ V_A \\ V_P \\ \vdots \\ V_P \\ I_F \\ 0 \end{bmatrix} = \begin{bmatrix} R_{1,1} & \cdots & R_{1,N} & R_{1,N+1} & \cdots & R_{1,N+M} & 0 & 0 \\ \vdots & \ddots & \vdots & \vdots & \ddots & \vdots & \vdots & \vdots \\ R_{N,1} & \cdots & R_{N,N} & R_{N,N+1} & \dots & R_{N,N+M} & 0 & 0 \\ R_{N+1,1} & \cdots & R_{N+1,N} & R_{N+1,N+1} & \cdots & R_{N+1,N+M} & 0 & 0 \\ \vdots & \ddots & \vdots & \vdots & \ddots & \vdots & \vdots & \vdots \\ R_{N+M,1} & \cdots & R_{N+M,N} & R_{N+M,N+1} & \cdots & R_{N+M,N+M} & 0 & 0 \\ 1 & \cdots & 1 & 0 & \cdots & 0 & 0 & 0 \\ 0 & \cdots & 0 & 1 & \cdots & 1 & 0 & 0 \end{bmatrix} \begin{bmatrix} I_1 \\ \vdots \\ I_N \\ I_{N+1} \\ \vdots \\ I_{N+M} \\ 0 \\ 0 \end{bmatrix} \quad (4)$$

A. *Soil Characterization*

We measured the soil resistivity using the Wenner Four-Electrodes Configuration method in two perpendicular directions (x and y axes, Fig. 4).

We repeated the measurements for six values of *a* (distance between two consecutive electrodes), in order to investigate soil resistivity at different depths.

The manufacturer of the measurement device gives, for the evaluation of uncertainty, the accuracy specification *A*, as in (5):

$$A = \pm 2\%\ of\ the\ reading\ value + 2\pi\ a \cdot 0.2 \qquad (5)$$

The measurements results are reported in *Fig. 3*, for the x and y axes. The graphs show that the resistivity decreases with an increase of the soil depth.

Since no significant differences appear between the two axes, we chose a simple two horizontal layers soil model, with the resistivity of the upper layer, ρ_1, greater than that of the second one, ρ_2.

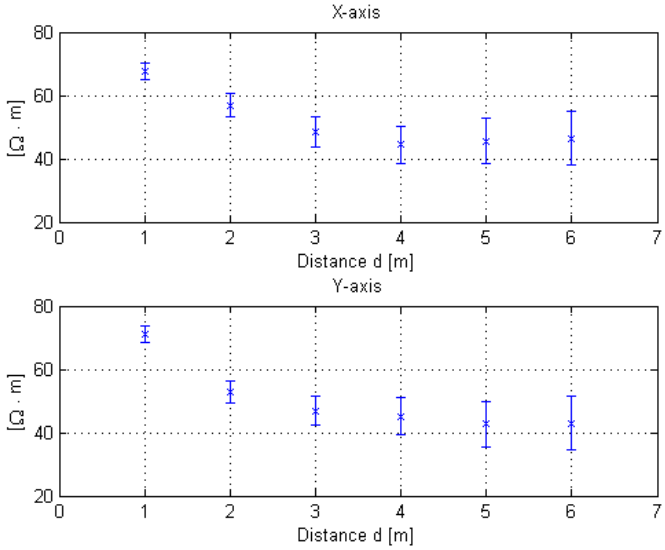

Fig. 3. Resistivity measurements along x and y axis

We computed the depth of the upper layer, h_1, and the resistivity values, ρ_1 and ρ_2, with the method described in [23], as follows. When $\rho_2 < \rho_1$, the finite expression for Wenner's apparent resistivity is reported in (6):

$$\rho_a = \rho_2 + (\rho_1 - \rho_2) \cdot \left[2 \cdot e^{-b(a)\cdot a} - e^{-b(2a)\cdot 2a}\right] \qquad (6)$$

where:

$$b = \frac{b_m - (b_m - 0.673191) \cdot e^{-0.479513 \cdot \frac{a}{h_1}}}{h_1} \qquad (7)$$

and

$$b_m = 1.33335 - 0.882645 \cdot \left(\frac{\rho_2}{\rho_1}\right)^{0.69706} \qquad (8)$$

The objective function to be minimized in order to obtain ρ_1, ρ_2 and h_1 is formulated as:

$$f(\rho_1, \rho_2, h_1) = \sum_{j=1}^{n} \left(\frac{\rho_j' - \rho_j(\rho_1, \rho_2, h_1)}{\rho_j'}\right)^2 \qquad (9)$$

where:

- n = number of electrode spacings for which apparent resistivity measurements are made;
- ρ_j' = measured apparent resistivity for jth electrode spacing;
- ρ_j= apparent resistivity at the jth electrode spacing computed by using finite expression (6).

In the model based on the Maxwell's sub-areas method, the first soil layer must include all electrodes so, in the optimization process, we imposed the inequality constraint $h_1 \geq 1\ m$ to respect this condition. The obtained parameters for the test site are reported in Table I.

TABLE I
DOUBLE SOIL HORIZONTAL LAYERS PARAMETERS

Symbol	Quantity	Values
ρ_1	upper layer resistivity	74 Ω ·m
ρ_2	lower layer resistivity	43 Ω·m
h_1	upper layer depth	1 m

B. *Ground Potential Distribution Measurements*

A 3D representation of the measurement site is shown in Fig. 4. The active electrode is an earth rod vertically driven in the ground, while the passive one is a horizontal bare conductor buried at 0.5 m depth.

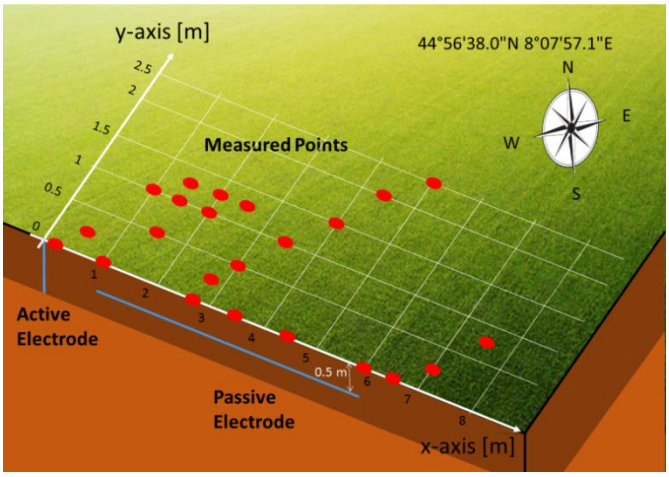

Fig. 4. Three-dimensional representation of the system of measurement

Different relative positions of the active electrode with respect to the passive one were tested. Here only the most interesting for the perturbation of the ground potential

distribution is reported. In all cases however the agreement between models and experimental measures was good.

An isolating transformer was used as generator to inject a current of 1 A in the active electrode. The earth current value was chosen considering the earth resistance of the active electrode (approximately 100 Ω) in order to reduce the risk associated to dangerous touch voltages. The Cartesian coordinates origin coincides with the center of the active electrode. The x axis coincides with the passive electrode axis.

Geometrical details are reported in Table II.

TABLE II
GEOMETRICAL DETAILS

Symbol	Quantity	Values
L_a	Length of active electrode	1·m
r_a	Active electrode radius	9·mm
L_p	Length of passive electrode	5 m
r_p	Passive electrode radius	4 mm
d_{a-p}	Distance between active and passive electrode	0.5 m

Fig. 5 represents the plan view of the soil surface; we stressed with a red circle the points in which we measured the electric potential. Next to each point, we reported the measured voltage values. Measurement uncertainties are lower than 2%, based on the multimeter specifications. The horizontal electrode was placed some weeks before the measurements, in order to let the soil settle after the excavation. The vertical rod, instead, was driven into the ground at the time of the measurements, slightly swinging around its axis due to the involuntary horizontal force. For this reason the contact between it and the ground was not perfect: a contact resistance should be taken into account in the models, [24].

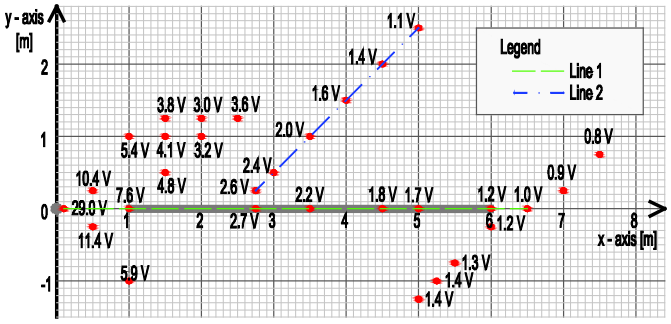

Fig. 5. Measured ground voltages and comparison lines

C. Comparison Between Computed and Measured Voltages

The previously described electrodes configuration was implemented in both the MaSM and FEM models. With the FEM model we simulated the cases with and without a thin layer (1 mm) with 1000 Ω m of resistivity all around the active electrode, in order to consider the contact resistance between the ground rod and the soil.

Two lines on the ground surface are used to compare the values of earth voltage, (Line 1 and Line 2 in Fig. 5). Also the EPR on the active electrode and the potential on the passive electrode (PEP) were compared. The results are presented in Fig. 6 and Table III. The results from MaSM and FEM models are nearly coincident: the three curves are superimposed in Fig. 6.

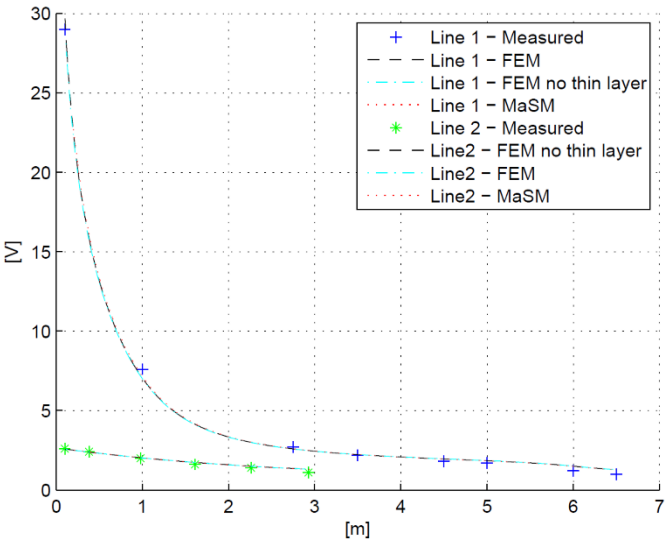

Fig. 6. Comparison between the MaSM, FEM and measured voltages

TABLE III
COMPARISON OF EPR AND PEP

Quantity	Measured	FEM	FEM no thin layer	MaSM
EPR	69.7	69.6	53.8	54.0
PEP	2.8	2.6	2.6	2.6

To evaluate how well the models fit the measured values, we calculated the coefficient of determination R^2, eq. (10), for each simulation.

$$R^2 = 1 - \frac{SS_{res}}{SS_{tot}} \tag{10}$$

where:

- SS_{res} is the sum of squares of residuals;
- SS_{tot} is the total sum of squares.

We also computed the coefficient R^2 considering the FEM model without thin layer as reference, in order to directly compare the models one to another. We report the results in Table IV.

TABLE IV
COEFFICIENT OF DETERMINATION R^2

Reference	FEM	FEM no thin layer	MaSM
Measurement	0.999	0.951	0.959
FEM no thin layer	-	-	0.999

The results show, generally, a fair agreement between measured and computed voltages. The only significant

difference lays in the EPR when the contact resistance is not considered.

A great accordance between the two models is always found, as demonstrated by the R^2 value, which is very close to one.

V. CASE STUDY

We applied the MaSM model to a realistic urban scenario, potentially candidate to be defined as a portion of GES. We considered as case study a portion of an urban district in Torino city center (45°03'34'' N 7°41'00'' E), highlighted with the red line in Fig. 7.

Fig. 7. Portion of an urban district considered for the simulation

The goal of the simulations is to evaluate how buried metallic parts, not connected to the ground-grid which injects a fault current into the ground, therefore defined as "floating metallic parts", modify the electrical potential on the soil surface with respect to the reference case in which only the ES of the MV/LV faulted substation is present. We considered four scenarios, characterized by different buried floating metallic parts (i.e. ESs of LV users, water pipes and tramway tracks) and described in Table V. For each scenario, the earth current is kept constant.

To carry out the comparison, together with contour plots of the ground potential, we used three shape coefficients evaluated on the same portion of soil surface: Uniformity (C_U), Valley Effect (C_{VE}), Gradient (C_G), which are described by equations (11), (12) and (13):

$$C_U = \frac{V_{AV}}{V_{MAX}} \tag{11}$$

$$C_{VE} = \frac{V_{MIN}}{V_{AV}} \tag{12}$$

$$C_G = \max(|\nabla V(x,y)|) \tag{13}$$

where:

- V_{AV} = Voltage Average;
- V_{MAX} = Maximum Voltage;
- V_{MIN} = Minimum Voltage;
- $|\nabla V(x,y)|$ = Absolut value of voltage gradient.

Moreover, we computed the Transferred Potentials (TPs) on LV ESs caused by the MV fault, evaluating if dangerous touch voltages can occur.

The prospective touch voltage (U_{vT}) is computed considering the induced potential on each LV ES and the earth potential profile in a delimited area around it.

To analyze the risk introduced by TPs, we used three parameters: Maximum Transferred Potential (TP_{MAX}), Maximum Touch Voltage ($U_{vT_{MAX}}$) and Maximum Earth Current (I_{50V}), respectively defined by (14), (15) and (16).

The last parameter is the maximum earth current $I_{E_{MAX}}$ that keeps the induced touch voltages lower than 50 V, the permissible touch voltage in a.c. LV systems.

$$TP_{MAX} = \frac{V_{TP_{MAX}}}{EPR} \tag{14}$$

$$U_{vT_{MAX}} = \max_j \left(\frac{V_{TP_j} - V_{S_j}}{EPR} \right) \tag{15}$$

$$I_{50V} = I_{E_{MAX}} \mid \left(V_{TP_j} - V_{S_j} \right) < 50V \quad \forall j \tag{16}$$

where:

- $V_{TP_{MAX}}$ = Maximum Voltage on the LV ESs in the district;
- V_{TP_j} = Transferred Voltage on the jth LV ES;
- V_{S_j} = Minimum Voltage on the Soil Surface for the Considered Area around the jth LV ES.

TABLE V
BURIED METALLIC PARTS CONSIDERED IN EACH SCENARIO

	Scenario N°			
Metallic parts	1	2	3	4
ES of the fault substation	✓	✓	✓	✓
ESs of LV users	-	✓	✓	✓
Water pipes	-	-	✓	✓
Tramway tracks	-	-	-	✓

A. Case Study Simulation

According to the requirements for the automatic disconnection of supply given by the international Standard IEC 60364-4 [8] for TT systems (the unique possible for LV users in Italy), each building has an ES disjointed from the MV/LV substation's one. The ESs of LV users, as well as the ES of the MV/LV substation in which the fault occurs, are modeled with a square electrode with side $L_{se} = 15\ m$, buried at 0.5 m under the soil level (red continuous lines in Fig. 8).

The ES of the faulted MV/LV substation is highlighted with the letter "F".

In the same figure, the blue dash-dot lines represent the water pipes while the green dashed lines represents the tramway tracks. The former are buried at 1 m and 1.3 m while the latter can be considered laying at the soil level.

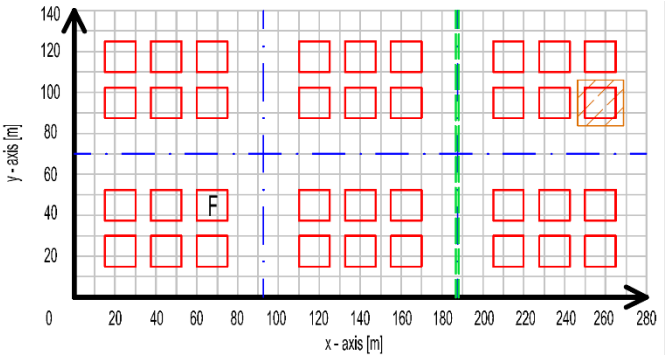

Fig. 8. Plan view of the implemented case study

The soil was considered homogeneous, characterized by a resistivity of 100 $\Omega \cdot m$.

Considering that the simulated system is linear, in order to carry out a per-unit analysis, we choose 100 A as earth current value I_E.

For the computation of the induced touch voltages, we considered the earth potential in a delimited area, constituted by a square of 22.5 m side, around each LV ES. In Fig. 8 the considered area for the LV ES with coordinates (65; 257.5) is stressed with sandy oblique dashed lines as an example.

Geometrical details are reported in Table VI.

TABLE VI
GEOMETRICAL DETAILS OF THE CASE STUDY

Symbol	Quantity	Values
L_{SE}	Length of square electrode	15 m
r_{SE}	Square electrode radius	4 mm
r_{WP}	Water pipes radius	50 mm
r_{TT}	Tramway tracks radius	60 mm

B. *Simulation Results*

We reported the EPR and the comparison parameters described in the paragraph above in Table VII, for the four simulated scenarios.

Fig. 9 - Fig. 13 show the contour plots of the ground potential.

TABLE VII
EPR AND SHAPE COEFFICIENTS FOR THE SIMULATED SCENARIOS

	Scenario N°			
Quantity	1	2	3	4
EPR [V]	391	386	379	379
C_U	0.089	0.090	0.091	0.091
C_{VE}	0.274	0.277	0.330	0.331
$C_G\ [V/m]$	70.021	70.843	70.327	70.329
$TP_{MAX}\ [\%]$	-	19.5	18.7	18.7
$U_{vT_{MAX}}$ [%]	-	7.5	7.6	7.6
$I_{50V}\ [A]$	-	173	174	174

The maximum difference in the EPR value is just 3.1 %. However, a descending trend can be noticed: the more the number of metallic parts, the lower is the EPR. Indeed, it can be said that from the point of view of the EPR, adding buried metallic parts is equivalent to increasing the soil conductivity.

The maximum variation in the uniformity coefficient C_U when adding buried metallic structures is 2.3 % (scenario 4), for the valley effect coefficient C_{VE} is 20.7 % (scenario 4) and for the gradient coefficient C_G is 1.2 % (scenario 2).

These coefficients give a global evaluation of the potential distribution on the soil surface: the slight increase in the coefficient C_U when considering additional buried metallic structures is mainly due to the increase in the exported potentials and in the reduction of the EPR; the same reasons can explain the increase in the coefficient C_{VE}; the increase in the potential gradient (even if very small) is mainly due to the imported low potentials in the area of the active ground-grid.

In Table VIII the same coefficients are recalculated for a single block of the urban area previously considered. In particular, the block involving the active ES is analyzed.

TABLE VIII
SHAPE COEFFICIENTS FOR A SINGLE BLOCK

	Scenario N°			
Quantity	1	2	3	4
C_U	0.225	0.227	0.214	0.214
C_{VE}	0.310	0.319	0.325	0.325
$C_G\ [V/m]$	70.021	70.843	70.327	70.329

The uniformity coefficients C_U calculated on the reduced area are obviously higher than those calculated before. The maximum voltage is in fact the same, while the average is higher (the low far-away potentials are not considered). The maximum difference between the scenarios remains low (5.1 %).

Also the valley effect coefficients C_{VE} are slightly higher if evaluated on a reduced area, and in this case the maximum difference between the scenarios is 4.9 %.

The gradient coefficients C_G are the same as those calculated on the overall test case area. This means that the points of maximum gradient were localized in proximity of the active ES.

As far as the TPs are concerned, the metallic parts with highest induced voltages are always the ESs identified by the coordinates (45, 45) and (65, 25) in Fig. 8. In fact, the factor that most influences the induced voltages is the distance between active and passive electrodes. A slight descending trend of TP_{MAX} can be noticed in the different scenarios: the more the number of metallic parts, the lower the transferred potentials. Probably, this effect is due to water pipes and tramway tracks that import a low potential in the area of the fault, considering that TPs can be calculated by superimposing the separate effect of all the electrodes (active and passive).

However, the maximum transferred potential TP_{MAX} is about 20% of the EPR for all the cases.

In the same area, we calculated the maximum induced prospective touch voltages $U_{vT_{MAX}}$, which is about 7.5 % of the EPR for all the scenarios (around 30 V for a fault current of

100 A). No significant differences among the scenarios can be noticed: probably, the reduction of TPs described before is compensated by the reduction in the potentials on the soil surface.

The maximum MV fault current that keeps induced touch voltages below 50 V (I_{50V}) is about 170 A for all the scenarios. In Italy, MV distribution systems are operated with their neutral point isolated from ground or with resonant earthing. In the first case, it is common to have fault currents bigger than I_{50V}, especially in an urban scenario where the network is more widespread [3]; in this case, considering that the fault can last for a certain time before being cleared [25] TPs can expose people to dangerous touch voltages. Instead, if the neutral point is connected to earth by Petersen coil, the fault current magnitude is reduced to around 50 A and, consequently, TPs are not dangerous.

In conclusion, the analyzed coefficients and the figures below (Fig. 9 -Fig. 13) support the idea that floating metallic parts do not significantly modify the ground potential distribution, and not necessarily in the direction of creating a quasi-equipotential area. Vice versa, in proximity of the active ES, they can introduce steeper gradient zones, thus reducing safety.

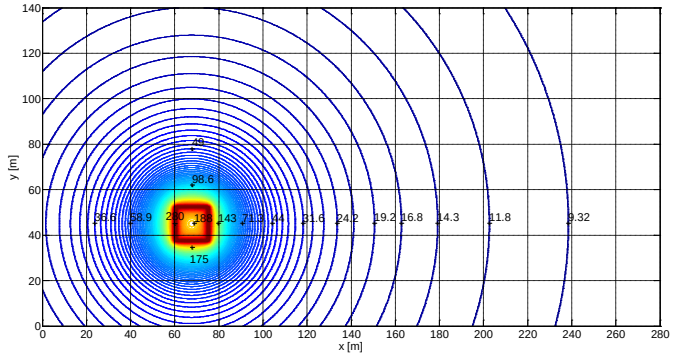

Fig. 9. Contour plot of the ground potential (in volt) for scenario 1 - only the ES of the faulted MV/LV substation is considered

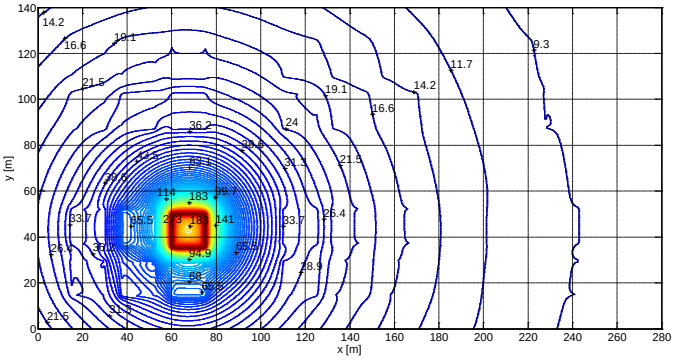

Fig. 10. Contour plot of the ground potential (in volt) for scenario 2 - the ESs of the faulted MV/LV substation and of LV users are considered

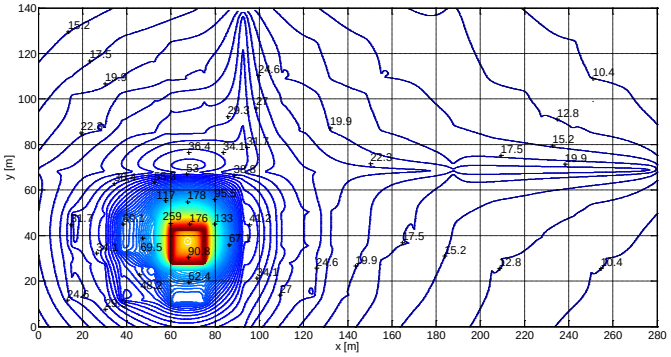

Fig. 11. Contour plot of the ground potential (in volt) for scenario 3 - ESs and water pipes are considered

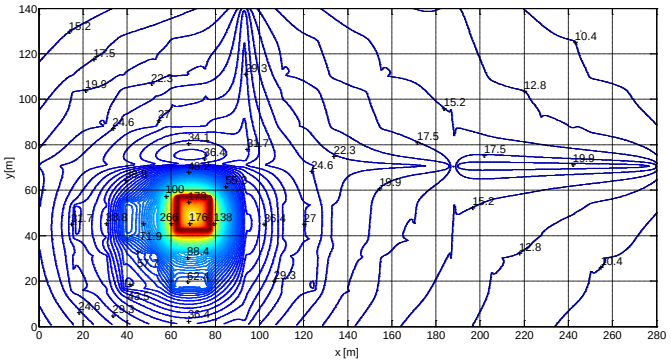

Fig. 12. Contour plot of the ground potential (in volt) for scenario 4 - ESs, water pipes and tramway tracks are considered

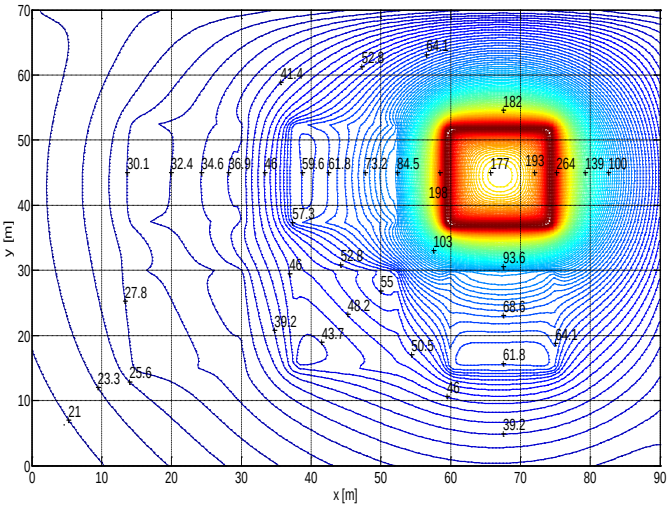

Fig. 13. Contour plot of the ground potential (in volt) for scenario 4 – detail

VI. CONCLUSION

In the definition of Global Earthing Systems, one of the aspects that is commonly stressed is the realization of a quasi-equipotential surface that should smooth the earth potential profile and that should avoid dangerous transferred potentials.

This effect should be due to the high number of interconnected ESs in the area and to the presence of other metallic parts, with different primary functions, such as water

and gas pipes, tramway tracks and building foundations. In this paper the second aspect is analyzed.

The simulation results show that when the additional buried metallic structures are not connected to the ESs, their influence on the ground potential distribution is not significant. The main changes in the ground potentials in fact take place only at a certain distance from the active ES, where the ground potential values are already low.

In addition to this, the results show that the potential gradients are worsened by buried metallic structures, in particular near the active ES: this means that the presence of floating metallic parts can introduce localized problems that otherwise were not present.

The comparison of the shape coefficients calculated on the overall test case area and on a reduced surface which includes the active ES suggests that buried metallic structures, not connected to the ESs, have two opposite effects: on one side, far away from the fault location, they tend to reduce the potential differences; on the other side, near the active ground-grid, they introduce low potentials, making the local situation worse.

For all the scenarios, the simulations show that dangerous potentials are transferred to LV ESs in the proximity of the MV/LV fault substation. Considering that the fault can last for a certain time before being cleared, TPs can expose people to dangerous touch voltages. Adding floating metallic parts does not significantly modify TPs.

In conclusion, buried metallic structures should not be considered in the practical procedure to certify the presence of a GES.

In order not to introduce localized problems, an important recommendation should be to interconnect all buried metallic structures to LV and MV ground-grids.

Further analysis will be carried out in future works, in order to evaluate the ground electric potential profile and TPs for different scenarios.

REFERENCES

[1] *Power installations exceeding 1 kV a.c., Part 1: Common rules*. EN 61936-1, 2011.

[2] *Earthing of power installations exceeding 1 kV a.c.* EN 50522, 2011.

[3] M. Mitolo, P. E. Sutherland, and R. Natarajan, "Effects of High Fault Currents on Ground Grid Design," *Industry Applications, IEEE Transactions on*, vol. 46, no. 3, pp. 1118–1124, 2010.

[4] R. Tommasini, E. Pons, and S. Toja, "MV ground fault analysis and global grounding systems," in *in Proceeding (448) IASTED Power and Energy Systems* , 2004.

[5] M. Desmedt, J. Hoeffelman, and D. Halkin, "Use of a global earthing system to implement the safety requirements for protecting against indirect contacts in HV systems," in *Electricity Distribution, 2001. Part 1: Contributions. CIRED. 16th International Conference and Exhibition on (IEE Conf. Publ No. 482)*, 2001, vol. 2, p. 10–pp.

[6] G. Parise, L. Martirano, and L. Parise, "Globality levels of grounding systems," in *Industrial \& Commercial Power Systems Tehcnical Conference (I\&CPS), 2014 IEEE/IAS 50th*, 2014, pp. 1–7.

[7] J. R. Dunki-Jacobs and C. St Pierre, "The function and composition of the global industrial grounding system," *Industry Applications, IEEE Transactions on*, vol. 42, no. 1, pp. 172–185, 2006.

[8] *Low-voltage electrical installations - Part 4-41: Protection for safety - Protection against electric shock*. IEC 60364-4, 2005.

[9] D. Garrett and K. Wallace, "A critical analysis of grounding practices for railroad tracks in electric utility stations," *Power Delivery, IEEE Transactions on*, vol. 8, no. 1, pp. 90–96, 1993.

[10] F. Freschi, M. Mitolo, and M. Tartaglia, "Interferences Phenomena Between Separate Grounding Systems," *IEEE TRANSACTIONS ON INDUSTRY APPLICATIONS*, vol. 50, no. 4, pp. 2853–2860, 2014.

[11] D. R. Doan, J. S. Fannon, H. L. Floyd, M. Scarborough, and others, "Railroad Tracks As A Potential Source Of Ignition In Hazardous (Classified) Locations," in *Petroleum and Chemical Industry Technical Conference, 2007. PCIC'07. IEEE*, 2007, pp. 1–5.

[12] I. Colominas, F. Navarrina, and M. Casteleiro, "Analysis of transferred earth potentials in grounding systems: A BEM numerical approach," *Power Delivery, IEEE Transactions on*, vol. 20, no. 1, pp. 339–345, 2005.

[13] J. C. Maxwell, *A Treatise On Electricity and Magnetism*, vol. 2. New York: Dover Publications, 1954.

[14] E. D. Sunde, *Earth conduction effects in transmission systems*. New York: Dover Publications, 1968.

[15] M. Sylos Labini, A. Covitti, G. Delvecchio, and C. Marzano, "A study for optimizing the number of subareas in the Maxwell's method," *Magnetics, IEEE Transactions on*, vol. 39, no. 3, pp. 1159–1162, 2003.

[16] R. Andolfato, L. Fellin, and R. Turri, "Analisi di impianti di terra a frequenza industriale: confronto tra indagine sperimentale e simulazione numerica," *ENERGIA ELETTRICA-MILAN-*, vol. 74, pp. 123–134, 1997.

[17] V. Cataliotti and A. Campoccia, *Impianti di terra*. TNE, 2013.

[18] F. Freschi, M. Mitolo, and M. Tartaglia, "An Effective Semianalytical Method for Simulating Grounding Grids," *Industry Applications, IEEE Transactions on*, vol. 49, no. 1, pp. 256–263, 2013.

[19] M. Bronzini, G. Delvecchio, N. Mitaritonna, P. Pugliese, and M. S. Labini, "A Method for Studying the Current Field Generated by Interconnected Grounding Systems," in *Computer Engineering in Applied Electromagnetism*, Springer, 2005, pp. 251–256.

[20] P. Buccheri, V. Cataliotti, and G. Morana, "Calcolo automatico di impianti di terra comunque complessi in terreni omogenei e non omogenei a doppio strato," *Energ. Elettr*, pp. 293–304, 1977.

[21] G. Ala, P. Buccheri, and A. Campoccia, "Interferenza tra elettrodi interrati rettilinei a caduta di tensione longitudinale non trascurabile. Analisi dell'accoppiamento conduttivo," *ENERGIA ELETTRICA-MILAN-*, vol. 69, pp. 405–405, 1992.

[22] M. Lorentzou, A. Kladas, and N. Hatziargyriou, "Finite element modelling of grounding systems considering electrode geometry effects," *Magnetics, IEEE Transactions on*, vol. 35, no. 3, pp. 1757–1760, 1999.

[23] H. R. Seedher and J. Arora, "Estimation of two layer soil parameters using finite Wenner resistivity expressions," *Power Delivery, IEEE Transactions on*, vol. 7, no. 3, pp. 1213–1217, 1992.

[24] J. Trifunovic and M. Kostic, "Analysis of influence of imperfect contact between grounding electrodes and surrounding soil on electrical properties of grounding loops," *Electrical Engineering*, vol. 96, no. 3, pp. 255–265, 2014.

[25] J. van Waes, F. Provoost, J. van der Merwe, J. Cobben, A. van Deursen, M. van Riet, and P. van der Laan, "Current distribution in LV networks during 1-phase MV short-circuit," in *Power Engineering Society Winter Meeting, 2000. IEEE*, 2000, vol. 4, pp. 2385–2390.

Enrico Pons received the master degree in electrical engineering and the Ph.D. degree in industrial safety and risk analysis from Politecnico di Torino, Torino, Italy. He is currently a postdoctoral research fellow there. He worked as a teaching assistant to several courses in Politecnico di Torino. His research activities include complexity in energy systems, power systems security, complex networks methodologies for

the analysis of power systems vulnerability and electrical safety. He co-authored more than 20 publications on various topics related to power systems and electrical engineering.

Pietro Colella received the Master's degree in electrical engineering from Politecnico di Torino, Turin, Italy. He is currently pursuing the Ph.D. degree in electrical engineering at the same institute. His research interest includes power systems and electrical safety. He is a Student Member of IEEE and AEIT.
Mr. Colella was a recipient of the CEI (Italian Electrotechnical Committee) "Best Thesis Award" in 2012.

Riccardo Tommasini received the master degree and the Ph.D. in electrical engineering. He is currently assistant professor at Politecnico di Torino, Italy. His research activities include power systems and electrical safety. He is member of CEI, the Italian Electrotechnical Committee where he is working in the 31 Committee, dealing with the evaluation of hazards due to the risk caused by explosive atmospheres and in committee 81, dealing with the protection against lightning.

Roberto Napoli graduated in Electrical Engineering in 1969. He is Full Power System Professor at Politecnico di Torino, Italy. His research interests include operation, planning, economics and security of electric energy systems as well as domotic, energy efficiency controls and electrical safety.

Pasquale Montegiglio received the Master's degree in electrical engineering from Politecnico di Bari, Bari, Italy. He is currently working as research assistant for the Electrical and Information Engineering Department (DEI) of the same institute. His research interest includes power systems, electrical safety, multiobjective optimization and differential evolution algorithms.

Giuseppe Cafaro received the degree summa cum laude in electrical engineering in 1976 from the University of Bari, Italy. From 1986 he worked at the same institute as Associate Professor and currently he is Associate Professor of Electrical Safety Techniques and Regulations at the Politecnico di Bari. His research interests also include electrical network theory, power system computing, planning and reliability.

Francesco Torelli received the degree in electrical engineering in 1966 from Politecnico di Milano, Milan, Italy. He is Professor of power systems and is responsible for the national research program on ancillary services sponsored by the Italian Ministry of Research. He joined the Electrical Engineering Department of the University of Bari, Bari, Italy as Assistant Professor and Associate Professor of power systems in 1966. His research main interests are in power system analysis and control.